

## Article

# Oral Bioavailability Enhancement of Vancomycin Hydrochloride with Cationic Nanocarrier (Leciplex): Optimization, In Vitro, Ex Vivo, and In Vivo Studies

Menna M. Abdellatif <sup>1,\*</sup> , Sara Mohamed Ahmed <sup>1</sup>, Mohamed A. El-Nabarawi <sup>2</sup> and Mahmoud Teaima <sup>2</sup> 

<sup>1</sup> Department of Industrial Pharmacy, College of Pharmaceutical Sciences and Drug Manufacturing, Misr University for Science and Technology, Giza 12566, Egypt

<sup>2</sup> Department of Pharmaceutics and Industrial Pharmacy, Faculty of Pharmacy, Cairo University, El-Kasr El-Aini Street, Cairo 11562, Egypt

\* Correspondence: menna.abdallatif@must.edu.eg; Tel.: +2-010-0564-7945

**Abstract:** To explore the performance of the cationic nanocarrier leciplex (LPX) in escalating the oral bioavailability of vancomycin hydrochloride (VAN) by promoting its intestinal permeability. With the aid of a D-optimal design, the effect of numerous factors, including lipid molar ratio, cationic surfactant molar ratio, cationic surfactant type, and lipid type, on LPX characteristics, including entrapment efficacy (EE%), particle size (P.S.), polydispersity index (P.I.), zeta potential value (Z.P.), and steady-state flux (J<sub>ss</sub>) were assessed. The optimized formula was further evaluated in terms of morphology, ex vivo permeation, stability, cytotoxicity, and in vivo pharmacokinetic study. The optimized formula was spherical-shaped with an E.E. of 85.2 ± 0.95%, a P.S. of 52.74 ± 0.91 nm, a P.I. of 0.21 ± 0.02, a Z.P. of + 60.8 ± 1.75 mV, and a J<sub>ss</sub> of 175.03 ± 1.68 µg/cm<sup>2</sup>/h. Furthermore, the formula increased the intestinal permeability of VAN by 2.3-fold compared to the drug solution. Additionally, the formula was stable, revealed good mucoadhesive properties, and was well tolerated for oral administration. The in vivo pharmacokinetic study demonstrated that the VAN C<sub>max</sub> increased by 2.99-folds and AUC<sub>0-12</sub> by 3.41-folds compared to the drug solution. These outcomes proved the potentiality of LPX in increasing the oral bioavailability of poorly absorbed drugs.

**Keywords:** cationic nanocarriers; oral bioavailability; vancomycin hydrochloride; intestinal permeability; leciplex; BCS class III



**Citation:** Abdellatif, M.M.; Ahmed, S.M.; El-Nabarawi, M.A.; Teaima, M. Oral Bioavailability Enhancement of Vancomycin Hydrochloride with Cationic Nanocarrier (Leciplex): Optimization, In Vitro, Ex Vivo, and In Vivo Studies. *Sci. Pharm.* **2023**, *91*, 1. <https://doi.org/10.3390/scipharm91010001>

Academic Editor: Susi Burgalassi

Received: 18 November 2022

Revised: 10 December 2022

Accepted: 15 December 2022

Published: 21 December 2022



**Copyright:** © 2022 by the authors. Licensee MDPI, Basel, Switzerland. This article is an open access article distributed under the terms and conditions of the Creative Commons Attribution (CC BY) license (<https://creativecommons.org/licenses/by/4.0/>).

## 1. Introduction

The pharmaceuticals' Biopharmaceutics Classification System (BCS) categorized oral quick-release drug formulations based on aqueous solubility, intestinal permeability, and dissolving properties [1]. However, BCS Class III pharmaceutical substances are mainly hydrophilic and have a low permeability profile [2]. Therefore, drugs in this class are usually administered via injections that are often painful and occasionally even risky as their oral bioavailability is too low. In addition, this class includes highly valuable therapeutic moieties such as peptides and RNA-based drugs; therefore, there is a demand to improve oral delivery systems for these drugs to provide more convenient and painless administration [3].

Various approaches have been applied to augment the intestinal permeability of class III, including loading the drug into a protective particulate carrier coated with target-specific ligands, or mediating site-specific delivery of the drug-carrier complex [4]. Therefore, numerous delivery systems have been developed for enhancing the oral bioavailability of class III drugs, including micro- and nanoparticles, nanoemulsions, and formulations containing absorption enhancers or hydrophobic ion pairs [5].

The intestinal absorption of drugs is primarily dependent on the transcellular pathway, while the paracellular pathway is the main route of some small hydrophilic molecules [6].

However, for high molecular weight drugs (macromolecules) such as peptides and RNA-based drugs, it is hard to be absorbed into the portal vein by the transcellular pathway. Moreover, the paracellular route, which refers to the passage of drugs through water-filled pores of the tight junction, is impossible. Instead, macromolecules are transported effectively and rapidly by M cells from the lumen to the underlying gut-associated lymphoid tissue by phagocytosis. However, the numbers of M cells are very limited in human intestines, accounting for less than 1% [7]. Moreover, these therapeutic moieties are exposed to hydrolytic and enzymatic degradation in the gastrointestinal tract (GIT). Therefore, the oral bioavailability of macromolecules is usually limited.

Therefore, the oral drug delivery system designed to enhance the oral absorption of macromolecules should be capable of protecting the drug from hydrolytic and enzymatic degradation in the harsh gastric milieu of the GIT, enhancing intestinal absorption and having mucus adhesion or penetrating aspects. Mucoadhesive systems can prolong drug residence time for absorption in the intestinal tract by avoiding mucociliary clearance. In contrast, mucus penetrating systems can rapidly pass through the unstirred layer to reach the intestinal epithelium for absorption [8].

The role of nanocarriers in improving the oral bioavailability of hydrophilic macromolecules was studied in several research papers where nanocarriers can entrap the active biomacromolecules into the matrix or the core to protect against degradation through the GIT lumen. In addition, nanocarriers can be taken up by epithelial cells (endocytosis; transcellular pathway) or M cells in Peyer's patches [9,10]. Nanocarriers can also entrap penetration enhancers or be decorated by ligands to enhance oral absorption [11].

Vancomycin hydrochloride (VAN) is a hydrophilic glycopeptide antibiotic with a high molecular weight of 1485.7 Da. It is used for prophylaxis and treating severe, life-threatening infections caused by Gram-positive bacteria, e.g., *Staphylococcus aureus* and other species [12]. Therefore, this drug was chosen as a model drug to prove the efficiency of nanocarriers in improving the oral bioavailability of a macromolecule drug belonging to class III.

The oral delivery of VAN is challenging as its oral bioavailability is limited by degradation in the stomach's acidic environment, intestinal enzymatic degradation, low epithelial permeability, and rapid clearance from the gastrointestinal tract (GIT) [13]. Therefore, the oral drug delivery system designed to enhance the oral absorption of VAN should be capable of protecting the drug from hydrolytic and enzymatic degradation in the GIT, enhancing intestinal absorption, and prolonging the residence of the drug in the GIT.

Several nanocarriers have been developed to enhance VAN oral delivery, such as polymeric nanoparticles, liposomes, self-emulsifying drug delivery systems (SEDDS), and inorganic nanoparticles. Loveymil et al. reported that coating VAN nanoparticles with a bioadhesive material could improve residence time and drug contact with epithelium, thus increasing intestinal drug permeability [14]. Zakeri-Milani et al. found that the VAN release from poly lactide-co-glycolide nanoparticles was more sustained than the physical mixture; moreover, the intestinal permeation of VAN was improved using nanoparticles [15]. Zaichik et al. developed a self-emulsifying drug delivery system (SEDDS) to increase the lipophilicity of VAN via hydrophobic ion-pairing with cetyltrimethylammonium bromide (CTAB) and thus increase the intestinal VAN permeability [16]. Additionally, Efiana et al. incorporated VAN into papain-palmitate-modified SEDDS through a hydrophobic ion pair formation to improve VAN intestinal mucus permeation and found that the using 0.5% papain-palmitate increased the mucus permeability of SEDDS [17]. Recently, Ndayishimiye et al. developed silica nanoparticles (SNPs)-based formulations to enhance the epithelial permeability of VAN. The research group found that VAN-loaded SNPs enhanced the permeability of VAN across an epithelial cell monolayer compared to the free drug solution [12]. Furthermore, Uhl et al. formulated tetraether lipid-stabilized liposomal nanocarriers decorated with cell-penetrating peptides to enhance the oral bioavailability of VAN via enhancing its mucosal permeation [18]. The previous research demonstrated that several nanocarrier systems had been modified to improve VAN oral bioavailability;

however, it is essential to develop a scalable, biocompatible, and simple-to-prepare drug delivery system that can offer a comparable improvement in VAN oral bioavailability.

Studies pointed out that intestinal permeation enhancers or bio-enhancers incorporated in nanocarriers may enhance the oral bioavailability of macromolecules by one or combined mechanisms of the following mechanisms: (a) altering the epithelial structure transiently, which leads to facilitated uptake of drugs; (b) higher fusion affinity of lipid vesicles with cell membranes; (c) opening of tight junctions that facilitate paracellular absorption of drugs [19]. Surfactants such as bile salts, cationic surfactants, and nonionic surfactants are mainly incorporated into nanocarrier formulae. Cationic surfactants have gained much attention as a bioenhancer as it improves cellular uptakes and mucoadhesion of the nanocarrier [20,21].

Leciplex (LPX) was chosen as a potential carrier to enhance the oral bioavailability of VAN as it is characterized by ease of scale-up, absence of the organic solvent, simplicity of preparation, and inherent enhanced stability [22]. LPX is a positively charged phospholipid-based vesicular system whose major components are phospholipid, a cationic surfactant, and a biocompatible solvent. The selection of LPX for augmenting intestinal permeability of VAN is based on its positive charge, which facilitates nanocarrier adhesion onto the negatively charged epithelial cell surfaces and increases cellular uptake of the loaded drug [23]. Moreover, previous studies also indicated the stability of positively charged vesicles in GIT as the positive surface can protect the surface of lipid-based vesicles, making it difficult for bile acid to reach the lipid bilayer [24,25]. In addition, the perceived advantage of small particle size ( $\leq 100$  nm) in increasing transmembrane permeability [26].

Currently, designs of experiments (DOE) have been commonly applied for the formulation and development of drug delivery systems as they reduce the number of experiments to be performed. The D-optimal design (DOD) is one of the techniques in the response surface method which decreases the number of experiments when there are some categorical; also, it finds the primary and interacting impacts of the mixture's component variables and reduces the projected run deviations [27,28]. Therefore, the DOD was used to explore and compare the effects of various variables on the characteristics of LPX.

## 2. Materials and Methods

### 2.1. Materials

Vancomycin hydrochloride (VAN) was donated from Kahira Pharmaceutical Co. (Cairo, Egypt). Phospholipon 90 G (PL-90 G) was purchased from Lipoid GmbH (Ludwigshafen, Germany). Soy phosphatidylcholine (SPC), cetyltrimethylammonium bromide (CTAB), dimethyldidodecylammonium bromide (DDAB), Roswell Park memorial institute (RPMI) media, sulforhodamine-B, tris aminomethane base, and mucin were received from Sigma-Aldrich Chemical Co. (St. Louis, MO, USA). Transcutol was obtained from Alfa Aesar (Kandel, Germany). All other reagents and solvents are of analytical grade.

### 2.2. Preparation of VAN-Loaded LPX

A single-step procedure was utilized to prepare LPX formulae with a different lipid:surfactant molar ratios (Table 1). First, lipids and surfactants were weighed and solubilized in Transcutol P in a shaker water bath (LWBS-A12, Labtron, Camberley, UK) at 70 °C until a clear yellow, homogenous solution was obtained. Next, the aqueous phase maintained at 70 °C containing 50 mg of VAN was added to the lipid mixture at once under cyclomixing (~1200 rpm) until a uniform dispersion was formed [29].

**Table 1.** DOD of VAN-loaded LPX.

Independent Variables for LPX Design	Levels	
	Low	High
X <sub>1</sub> : lipid molar ratio	0	1
X <sub>2</sub> : cationic surfactant molar ratio	1	5
X <sub>3</sub> : cationic surfactant type	SPC	PL-90 G
X <sub>4</sub> : lipid type	CTAB	DDAB

Abbreviations: DOD; D-optimal design, CTAB; Cetrimonium bromide, DDAB; Dimethyldioctadecylammonium bromide, SPC; Soya phosphatidylcholine, PL-90 G; Phospholipon 90 G.

### 2.3. Characterization of VAN-Loaded LPX

#### 2.3.1. Determination of Entrapment Efficiency (E.E.%)

Determination of the E.E.% of VAN by membrane dialysis technique. Briefly, 1 mL of LPX formula was placed in the dialysis bag (M.W. of 12,000–14,000 Dalton), suspended in a beaker containing 100 mL of distilled water. Then, aliquot samples were withdrawn at various intervals, and VAN content was determined by analysis at 280 nm using a UV-spectrophotometer (UV-1650; Shimadzu Corp., Kyoto, Japan). The following equation was used to calculate the E.E. percent [30]:

$$\text{E.E. (\%)} = \frac{\text{Total VAN amount} - \text{Diffused VAN amount}}{\text{Total VAN amount}} \times 100 \quad (1)$$

#### 2.3.2. Determination of Particle Size, Polydispersity Index, and Zeta Potential

The mean hydrodynamic diameter (z-average), P.I., and surface charge of the LPX formulae were determined based on Dynamic Light Scattering (DLS) using Malvern Zetasizer NanoZS. (Zetasizer Nano Series, Malvern, UK) at 25 °C. Before analysis, samples were diluted with double-distilled water to a suitable concentration [31].

#### 2.3.3. In Vitro Drug Release Study

The in vitro drug release of Van loaded-LPX formulae was studied using the Franz diffusion cell. Phosphate buffer (PBS, pH 7.4) was used as a release medium. The cellulose membrane (molecular weight cutoff 12,000 Da) was soaked in distilled water for 12 h before use. Two mL of the LPX formula (10 mg VAN) was poured into the donor cell. The receptor cell was filled with 50 mL of release media and maintained at 37 °C and 50 rpm. An aliquot of 0.5 mL was removed at various points, and the same volume of fresh media was added accordingly. The drug content of the samples was analyzed spectrophotometrically at 280 nm. The cumulative amount of VAN release was plotted as a function of time. The flux of VAN at a steady state ( $J_{ss}$ ;  $\mu\text{g}/\text{cm}^2/\text{h}$ ) was calculated from the slope of the linear portion [32]. To understand the drug release mechanism of LPX formulae, different kinetics models such as zero order, first order, Higuchi model, and Korsmeyer -Peppas model were evaluated. The fitted model was determined based on the maximum value of the correlation coefficient ( $R^2$ ).

### 2.4. Optimization of VAN-Loaded LPX Formulations

A DOD experiment was conducted using Design Expert<sup>®</sup> software version 7 (Stat Ease, Inc., Minneapolis, MN, USA) to examine the impact of various parameters on the formulation of LPX. In the design of the LPX formulation, the four evaluated parameters were (X<sub>1</sub>: lipid molar ratio), (X<sub>2</sub>: cationic surfactant molar ratio), (X<sub>3</sub>: cationic surfactant type) at two levels, and (X<sub>4</sub>: lipid type) at two levels. The dependent variables for both designs were the E.E.% (Y<sub>1</sub>), P.S. (Y<sub>2</sub>), P.I. (Y<sub>3</sub>), Z.P. (Y<sub>4</sub>), and  $J_{ss}$  (Y<sub>5</sub>).

### 2.5. Selecting the Optimized VAN-LPX Formula

The desirability tool, which allowed for simultaneous assessment of each response, was used to select the optimized formula. The basis for choosing the optimized formula was to produce the smallest P.S., P.I., maximum J<sub>ss</sub>, EE %, and Z.P. values.

### 2.6. Morphology of the Optimized VAN-LPX Formula

The shape of the LPX nanocarrier was determined with transmission electron microscopy (TEM) (JEM-1230, Joel, Tokyo, Japan) using negative staining [31].

### 2.7. Ex Vivo Permeation Study via Non-Everted Intestinal Sac Model

The intestinal sac was excised after the abdomen of a sacrificed rabbit was cut open. The lumen of the sac was thoroughly rinsed by the passage of ringer solution through it repeatedly until there was no fecal matter left in the lumen of the sac. The intestinal sac was then sealed at one end without damaging the tissue. A half mL of VAN solution or the formula (equal to 2.5 mg of VAN) was dropped into the rabbit intestine with the help of a micropipette, and the other end of the sac was also sealed. The intestinal sac containing the test sample was placed in a 20 mL ringer solution at 37 °C. At definite intervals, 0.5 mL of receiver media was removed, and the same fresh media volume was added to the receiver chamber. The permeated amount of VAN was determined using HPLC, where the C<sub>18</sub> column was used with a mobile phase consisting of buffer citrate (pH 4): acetonitrile: methanol in the ratio of 85: 10: 5 (v/v/v) as the mobile phase at a flow rate of 1.0 mL/min and U.V. detection at 280 nm. The apparent permeability was calculated as the amount (μg) of VAN, permeation per intestinal mucosa surface area (cm<sup>2</sup>), according to the following equation [33]:

$$\text{Apparent permeability} = \Delta Q / (\Delta t \times A \times C_0) \text{ (cm/h)} \quad (2)$$

where  $\Delta Q / \Delta t$  was the flux across the intestinal sac (μg/h), A was the surface area of the sac (cm<sup>2</sup>), and C<sub>0</sub> was the initial drug concentration (μg/mL).  $\Delta Q$  was cumulative drug penetration (μg/cm<sup>2</sup>).

### 2.8. Differential Scanning Calorimetry

The thermal behaviors of the individual components of the LPX formula and the selected formula of LPX were studied by differential scanning calorimetry (DSC 204 F1, Netzsch, Germany). The samples were correctly weighed into standard aluminum pans. Thermograms were recorded during heating, and cooling runs at a scan rate of 10 °C min<sup>-1</sup> between 25 and 300 °C.

### 2.9. Effect of Storage on the Selected LPX Formula

The LPX formula stability was examined to verify its ability to keep its size and charge throughout the storage period. The formula was stored at 4 °C for three months before being assessed by contrasting its P.S., P.I., and Z.P. with a fresh formula. In addition, the stability of the LPX formula against enzymatic degradation was tested at the simulated gastric fluid (SGF) and simulated intestinal fluid (SIF) at 37 °C. A modified method was used to assess the amount of VAN retained after incubation with SGF and SIF due to the difficulty of separation of the LPX formula from the media due to its size; therefore, 1 mL of the formula was mixed with either 1 mL of SGF or SIF and placed in the dialysis bag, which was sealed and then placed in 100 mL distilled water for 2 h and stirred at 100 rpm; then, an aliquot of 0.5 mL was withdrawn from the distilled water and analyzed at 280 nm using a UV-spectrophotometer to determine the amount of the drug retained in the formula at a different pH.

### 2.10. Evaluation of Mucoadhesion Properties of the Selected Formula

The mucoadhesive nature of the prepared LPX was evaluated by examination of their interaction with the negatively charged mucin. In brief, the mucin aqueous solution was prepared and mixed with equal volume with the prepared LPX at 37 °C. Then, the Z.P. values of the mixtures were measured using Zetasizer Nano Z.S. (Malvern Instruments Ltd., UK) [30].

### 2.11. Cytotoxicity Assay

A Colorectal cancer cell line (CaCo-2) was provided by Nawah Scientific Inc. (Mokatam, Cairo, Egypt). Cells were kept in Roswell Park memorial institute (RPMI) media supplemented with 100 mg/mL of streptomycin, 100 units/mL of penicillin, and 10% heat-inactivated fetal bovine serum in humidified, 5% (*v/v*) CO<sub>2</sub> atmosphere at 37 °C. Sulforhodamine B (SRB) colorimetric assay was used to evaluate cell viability and performed in 96-well plates. In brief, cells were seeded at density  $5 \times 10^3$  cells/well overnight and then treated with the indicated concentrations of different formulations for 72 h. The cells were fixed by replacing media with 150 µL of 10% trichloroacetic acid (TCA) and refrigerated at 4 °C for 1 h. Next, the supernatant was separated, and the plates were washed with water and air-dried. Next, 70 µL of SRB solution was added to each well and kept in a dark place at room temperature for 30 min. Plates were washed with 1% acetic acid and air-dried overnight. Then, bound SRB was solubilized with 150 µL tris aminomethane base (10 mM), and the plate was shaken for 5 min. The absorbance was measured at 540 nm using a BMG LABTECH®-FLUOstar Omega microplate reader (Ortenberg, Germany) [34].

### 2.12. In Vivo Assessment of the Selected LPX Formula

The Research Ethics Committee of the Faculty of Pharmacy at Cairo University approved animal studies (Approval no. PI 2842). The animal studies were conducted strictly with Animal Research: Reporting of In Vivo Experiments (ARRIVE) guidelines.

Twenty-four Wistar albino rats (weighing  $200 \pm 20$  g) were obtained from the breeding unit of the faculty of veterinary medicine at Cairo University. Throughout the investigation, complete adherence to all guiding standards for the care and management of laboratory animals was maintained. Animals were housed in cages at room temperature  $25 \pm 2$  °C and relative humidity of 50–60% under a 12 h light/dark cycle. The rats had free access to water but were denied food for 24 h before the experiment. The rats were divided into two groups, with 12 rats in each group, Group 1 drug aqueous dispersion and Group 2 LPX selected formula. The formulation and the VAN aqueous dispersion were administered orally (dose 20 mg/Kg) [35]. Under ether anesthesia, blood samples (0.5 mL) were collected into heparinized plastic centrifuge tubes using 0.8–1.1 mm capillary glass tubes at 0.5, 1, 2, 3, 4, 5, 6, 7, 8, and 12 h. The samples were centrifuged, and 200 µL of plasma was uptaken by a pipettor and mixed with the same volume of methanol to precipitate proteins. The mixture was stirred on a vortex mixer for 90 s and centrifuged at 9000 rpm for 10 min. Then, 20 µL of the supernatant was analyzed by an HPLC method [12]. Plasma concentration-time data of VAN were analyzed by a non-compartmental pharmacokinetic model using Kinetica software (version 4.4.1). The peak plasma concentration ( $C_{max}$ ) and the time of its occurrence ( $T_{max}$ ) were calculated from the concentration-time data. The linear trapezoidal rule determined the area under the plasma concentration-time curve (AUC) from time zero to the last time recorded ( $AUC_{0-t}$ ). The mean residence time (MRT) was also calculated. Data were statistically analyzed by unpaired *t*-test (two-tailed).

### Statistical Analysis of Data

Statistical analysis was completed using the software (GraphPad instat software, version 3.1, Dotmatics, Boston, MA, USA). The results are expressed as the mean  $\pm$  S.D. Statistical investigations were achieved using the *t*-test and one-way analysis of variance (ANOVA), followed by the Tukey post-hoc test with *p*-values set at  $<0.05$ .

### 3. Results and Discussion

#### 3.1. Design Optimization

The basic LPX formulation contains phospholipid and cationic agents as the principal constituent in a specific ratio. Here, formulations were prepared using varied ratios and types of phospholipids and surfactants. LPX formulae were prepared and characterized to study the impact of several independent variables on the dependent variables, as seen in Table 2. Noticing the design analysis values in Table 3.

**Table 2.** Experimental runs, independent variables, and measured response of the DOD of VAN-loaded LPX.

Formulation Code	Lipid Molar Ratio (X <sub>1</sub> )	Surfactant Molar Ratio (X <sub>2</sub> )	Surfactant Type (X <sub>3</sub> )	Lipid Type (X <sub>4</sub> )	E.E.% (Y <sub>1</sub> )	P.S. (nm) (Y <sub>2</sub> )	P.I. (Y <sub>3</sub> )	Z.P. (mV) (Y <sub>4</sub> )	Jss (µg/cm <sup>2</sup> /h) (Y <sub>5</sub> )
F1	5	0	DDAB	SPC	99.33 ± 1.5	194.5 ± 1.75	0.26 ± 0.008	−64.4 ± 0.55	36.05 ± 0.49
F2	2	0.5	DDAB	PG90	81.6 ± 1.8	28.32 ± 1.15	0.29 ± 0.002	57.1 ± 1.1	166.23 ± 0.55
F3	1	1	DDAB	PG90	75.6 ± 1.2	18.51 ± 0.77	0.19 ± 0.005	64.9 ± 0.45	187.41 ± 1.20
F4	5	1	CTAB	PG90	94.0 ± 1.5	156.0 ± 1.59	0.40 ± 0.025	55.9 ± 1.35	102.61 ± 0.42
F5	3	0	CTAB	SPC	93.3 ± 1.1	96.48 ± 1.24	0.26 ± 0.005	−52.9 ± 0.89	136.08 ± 0.05
F6	5	1	DDAB	PG90	90.9 ± 0.78	147.0 ± 0.94	0.23 ± 0.043	52.3 ± 0.96	156.0 ± 0.96
F7	3	0.5	DDAB	SPC	94.4 ± 0.60	68.47 ± 0.85	0.24 ± 0.010	−29.3 ± 0.35	102.15 ± 1.10
F8	3	0	DDAB	PG90	88.2 ± 1.0	103.0 ± 0.55	0.51 ± 0.020	10.5 ± 1.20	113.28 ± 1.19
F9	5	0	DDAB	SPC	96.99 ± 1.7	189.3 ± 1.75	0.24 ± 0.018	−66.8 ± 0.41	37.72 ± 0.89
F10	1	0	CTAB	PG90	92.0 ± 1.7	102.2 ± 2.1	0.31 ± 0.028	19.8 ± 0.25	142.98 ± 0.69
F11	1	1	CTAB	SPC	91.2 ± 1.4	49.17 ± 0.28	0.28 ± 0.018	33.6 ± 0.30	178.44 ± 0.31
F12	5	1	CTAB	SPC	96.8 ± 1.41	121.2 ± 0.66	0.26 ± 0.051	−33.2 ± 1.4	141.25 ± 0.17
F13	1	1	DDAB	SPC	91.9 ± 0.81	73.85 ± 1.35	0.33 ± 0.030	42.3 ± 0.95	133.72 ± 0.5
F14	1	0	DDAB	SPC	95.6 ± 1.3	148.4 ± 0.22	0.26 ± 0.002	−49.4 ± 0.6	58.37 ± 0.26
F15	2	0.5	CTAB	SPC	95.0 ± 1.1	83.54 ± 1.23	0.34 ± 0.008	22.1 ± 1.05	160.69 ± 0.48
F16	5	0	CTAB	PG90	93.4 ± 1.2	162.4 ± 1.30	0.41 ± 0.046	3.05 ± 0.19	76.63 ± 0.45
F17	1	0	CTAB	PG90	89.6 ± 1.9	102.2 ± 1.69	0.31 ± 0.022	19.8 ± 0.15	142.98 ± 0.69
F18	3	0.5	CTAB	PG90	87.2 ± 1.3	61.7 ± 1.35	0.38 ± 0.005	38.2 ± 0.65	149.63 ± 0.43
F19	5	1	DDAB	PG90	91.4 ± 1.9	140 ± 1.52	0.35 ± 0.001	50.6 ± 0.25	161.24 ± 0.16

Abbreviations: E.E.%, entrapment efficiency percentage; P.S., particle size; P.I., polydispersity index; Z.P., zeta potential; Jss; steady-state flux, LPX; leciplex.

**Table 3.** Output data of the DOD analysis of LPX formulations and predicted and observed values for the selected LPX formula.

Source	E.E.% (Y <sub>1</sub> )	P.S. (nm) (Y <sub>2</sub> )	P.I. (Y <sub>3</sub> )	Z.P. (mV) (Y <sub>4</sub> )	Jss (µg/cm <sup>2</sup> /h) (Y <sub>5</sub> )
p-value	<0.0001	0.0016	0.1982	<0.0001	<0.0001
Model	2 FI	Quadratic	-	Linear	Quadratic
X <sub>1</sub> = A = Lipid molar ratio	<0.0001	0.0004	0.0962	0.0008	<0.0001
X <sub>2</sub> = B = surfactant molar ratio	0.0381	0.0043	0.2669	<0.0001	<0.0001
X <sub>3</sub> = C = surfactant type	0.3271	0.8949	0.9691	0.5983	<0.0001
X <sub>4</sub> = D = Lipid type	<0.0001	0.1166	0.1360	<0.0001	<0.0001
Adequate precision	19.724	10.43	4.53	19.791	42.568
R <sup>2</sup>	0.9636	0.84	0.33	0.9132	0.9969
Adjusted R <sup>2</sup>	0.9226	0.76	0.14	0.8884	0.9907
Predicted R <sup>2</sup>	0.8496	0.6	−0.26	0.8332	0.9044
Significant factors	X <sub>1</sub> , X <sub>2</sub> , X <sub>4</sub>	X <sub>1</sub> , X <sub>2</sub>	-	X <sub>1</sub> , X <sub>2</sub> , X <sub>4</sub>	X <sub>1</sub> , X <sub>2</sub> , X <sub>3</sub> , X <sub>4</sub>
Predicted value of the selected formula	87.38	50.98	0.22	65.1	178.41
Observed value of the selected formula	85.20 ± 0.95	52.74 ± 0.91	0.21 ± 0.02	60.8 ± 1.75	175.03 ± 1.68
The regression equation of the fitted model	+91.50 + 3.47\1 A−1.23 × B + 0.44 × C−3.84 × D + 1.92 × A\1 B−1.48\1 A\1 C + 1.34\1 A\1 D + 0.27\1 B\1 C 0.95\1 B\1 D + 1.61 × C × D	+106.80 + 43.44\1 A−21.6\1 B−2.16\1 C−6.84\1 D	-	+9.3017.03\1 A + 29.73\1 B + 1.67 × C + 28.76 × D	+126.49−20.74\1 A + 23.12\1 B + 8.84 \1 C + 7.92\1 D + 1.58\1 A\1 B6.16\1 A\1 C−5.24\1 A\1 D−12.03\1 B \1 C−3.62\1 B\1 D−20.32 1 C\1 D

Abbreviations: E.E.%, entrapment efficiency percentage; P.S., particle size; P.I., polydispersity index; Z.P., zeta potential; Jss; steady-state flux.

### 3.2. Effect of Formulation Variables on the Entrapment Efficiency%

The E.E.% for LPX was evaluated by the dialysis method. In the dialysis method, the un-entrapped drug is expected to diffuse out into a media. In contrast, the encapsulated drug remains entrapped inside the vesicles until it is released from the system. Figure 1 shows that the independent variables  $X_1$ ,  $X_2$ , and  $X_4$  significantly impact the E.E.% of VAN in the LPX formulae. Table 2 displays the E.E.% of the VAN LPX formulae, which ranged from  $75.6 \pm 1.2$  to  $99.33 \pm 1.5\%$ . The results demonstrated that the lipid molar ratio ( $X_1$ ) significantly E.E.% ( $p < 0.0001$ ). These findings concur with Date et al., who found that the E.E.% was increased by increasing the lipid molar ratio due to the formation of more rigid vesicles capable of encapsulating hydrophilic drugs and minimizing their leakage [36].

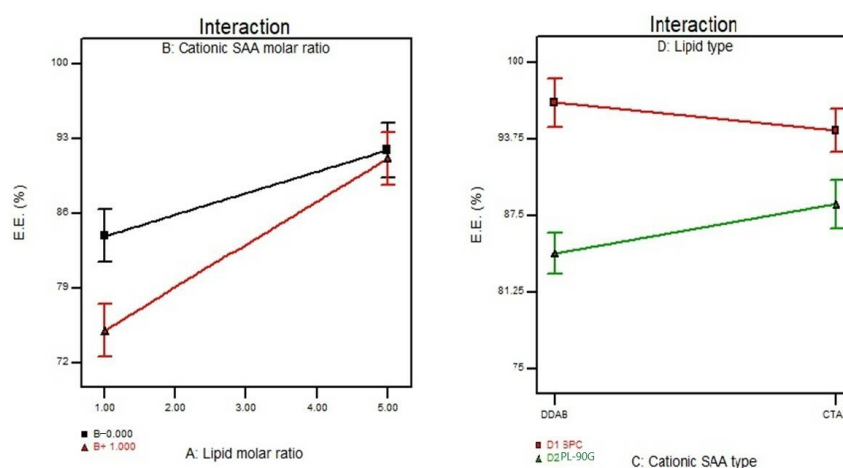


**Figure 1.** The effect of lipid molar ratio ( $X_1$ ), cationic surfactant molar ratio ( $X_2$ ), cationic surfactant type ( $X_3$ ), and lipid type ( $X_4$ ) on E.E.%. Abbreviation: E.E.%, entrapment efficiency percent.

On the contrary, increasing the cationic surfactant concentration reduced E.E.% ( $p = 0.0381$ ). These results might be due to the solubilization of phospholipids by the surfactant, leading to drug leakage from LPX. These results agree with Salama et al., who found that spironolactone encapsulation efficiency significantly decreased at increased surfactant concentration [37]. Additionally, the lipid type ( $X_4$ ) had a significant influence ( $p < 0.0001$ ) on the E.E.% of LPX, in which the highest E.E.% was found in LPX with SPC rather than PL-90 G, which could be attributed to the difference in the structure between them where SPC contains a percentage of saturated fatty acid. Hence, it forms a rigid matrix capable of decreasing drug leakage from the LPX formulae. At the same time, the PL-90 G composite of unsaturated fatty acid leads to a less rigid matrix allowing hydrophilic drug leakage from the nanocarriers. These results agree with Eroğlu et al., who found that unsaturated phospholipids were relatively more flexible and thereby provided less hindrance for the drug to be retained in the lipid bilayer [38]. Furthermore, the difference in the surface charge between SPC and PL-90 G might also affect the E.E.% of the positively charged drug (VAN) as SPC has a negative charge at neutral pH while PL-90 G has almost zero charges; based on this, it was expected that LPX obtained higher E.E.% values formulated with SPC due to electrostatic interactions between negatively charged phospholipid (SPC) and the positively charged drug (VAN) [39].

### 3.3. Effect of Formulation Variables on the Particle Size

The P.S. greatly affects intestinal permeability as the smaller nanocarriers enhance drug absorption through endocytosis and paracellular pathways. The P.S. of LPX formulae ranged from  $18.51 \pm 0.77$  to  $194.50 \pm 1.75$  nm, as displayed in Table 2. ANOVA results provided that both  $X_1$  and  $X_2$  significantly influenced the P.S. of the cationic nanocarrier, as shown in Figure 2. Where increasing lipid concentration resulted in larger vesicles, these results might be correlated with the E.E.% outcomes where increasing lipid molar ratio

led to a significant enhancement in the hydrophilic drug entrapment, thus forming larger vesicles. Adding a cationic surfactant to LPX formulae resulted in a significant reduction in P.S. due to steric repulsion provided by surfactant molecules, which prevents or decreases vesicle aggregation. It might also be ascribed to a decrease in the aqueous-lipid interfacial tension, which results in the creation of smaller vesicles or due to lipid solubilization by surfactant, leading to drug leakage from LPX leading to a smaller P.S. These findings correlate with Khatoona et al., who found that the high surfactant and low phospholipid concentration resulted in small-size vesicles [40].

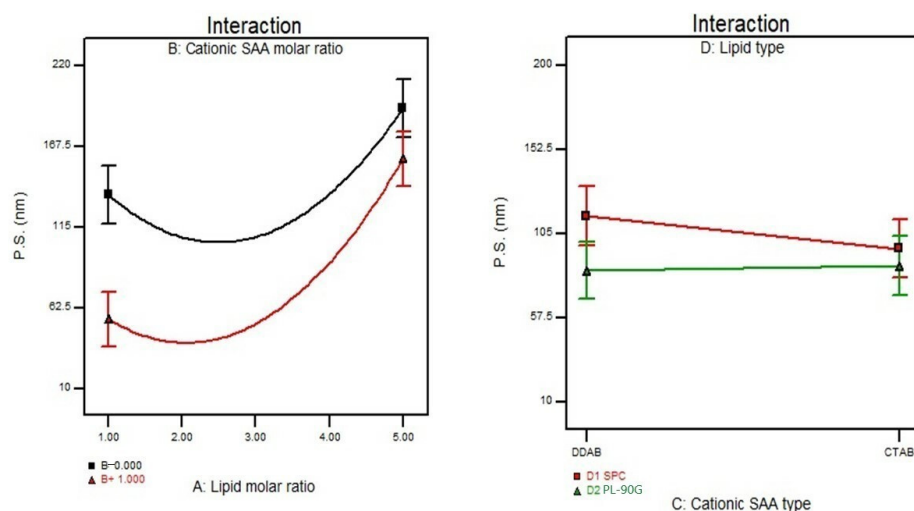


**Figure 2.** The effect of lipid molar ratio ( $X_1$ ), cationic surfactant molar ratio ( $X_2$ ), cationic surfactant type ( $X_3$ ), and lipid type ( $X_4$ ) on P.S. Abbreviation: P.S., particle size.

### 3.4. Effect of Formulation Variables on the Polydispersity Index

The P.I. values for all LPX formulae were lower than 0.5. Upon analysis of the effect of the independent factors on P.I. ( $Y_3$ ), no significant model fitted the data.

### 3.5. Effect of Formulation Variables on the Zeta Potential

The value of Z.P. is usually used as an indicator to predict the stability of the colloidal dispersion. As shown in Table 2, the Z.P. values for the LPX formulae ranged from  $-66.8 \pm 0.41$  to  $+64.9 \pm 0.45$  mV. The Z.P. of the prepared LPX was significantly influenced by  $X_1$ ,  $X_2$ , and  $X_4$ , as shown in Figure 3. The lipid molar ratio ( $X_1$ ) showed a significant impact on the Z.P. values where the LPX formula (F5) was composed of 3:0 (SPC: cationic surfactant) on increasing the lipid molar ratio to 5:0 (F1) using the same type of phospholipid the value increased from  $-52.9 \pm 0.89$  to  $-66.8 \pm 0.41$  mV. The addition of the cationic surfactant affected the prepared LPX formula's Z.P. values as it decreased the surface charge's negativity. The preference for positive charge in these formulations is to increase electrostatic interaction between cationic LPX and the mucus layer, facilitating the mucous adhesion of the LPX nanoparticles, which might prolong the residence time and drug contact with the underlying epithelium. Additionally, increasing the surfactant's molar ratio ( $X_2$ ) increased the Z.P. values and developed more stable nanovesicles. Additionally, the lipid type ( $X_4$ ) showed a significant effect on Z.P. values with  $p$  values of  $<0.0001$ ; all formulae containing SPC without cationic surfactant showed negative Z.P. values due to the orientation of phosphate groups at the exterior [41]. On the contrary, PL-90 G showed a low positive surface charge which could be attributed to unsaturated fatty acid lipids leading to leakage of the positively charged drug, as PL-90 G has a zero charge at the neutral pH, as mentioned before.

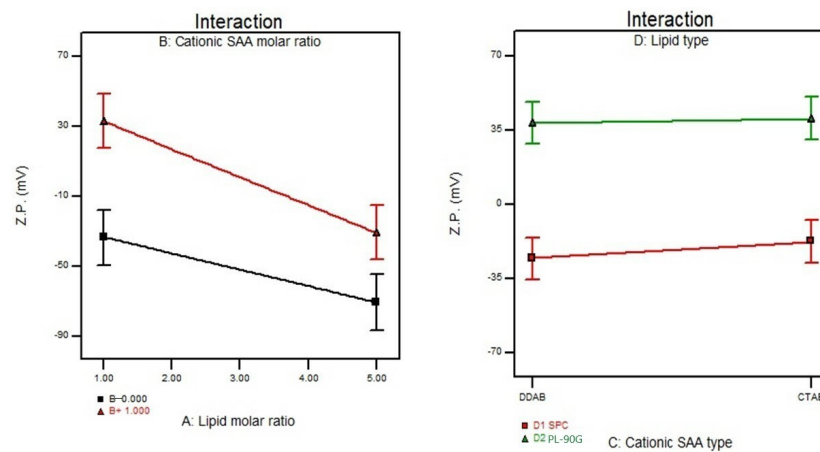


**Figure 3.** The effect of lipid molar ratio ( $X_1$ ), cationic surfactant molar ratio ( $X_2$ ), cationic surfactant type ( $X_3$ ), and lipid type ( $X_4$ ) on Z.P. Abbreviation: Z.P., zeta potential.

### 3.6. Effect of Formulation Variables on the In Vitro Drug Release

The in vitro drug release from different LPX formulae was represented as  $J_{ss}$ . The values of  $J_{ss}$  of the drug from the nanocarriers ranged from  $36.06 \pm 0.49$  to  $187.41 \pm 1.2 \mu\text{g}/\text{cm}^2/\text{h}$ , as displayed in Table 2. ANOVA results provided that  $X_1$ ,  $X_2$ ,  $X_3$ , and  $X_4$  significantly influenced the release of the prepared LPX, as displayed in Figure 4. The  $J_{ss}$  values decreased as the lipid concentration increased due to a decrease in the bilayer malleability, increased rigidity of vesicles, and increased medium viscosity. This may be slow drug diffusion into the dissolving media [29]. On the contrary, the  $J_{ss}$  values increased on increasing the surfactant concentration; this might be due to the formation of smaller vesicles and, thus, increased surface area. Adding the more hydrophobic surfactant DDAB (log p 11.8) reduced the values of the  $J_{ss}$  compared to the less hydrophobic surfactant CTAB (log p 8). The lipid type ( $X_4$ ) affected the values of  $J_{ss}$  as PL-90 G increased the  $J_{ss}$  values more than SPC. These results might be due to the difference in the fatty acid saturation between PL90 G and SPC. These results agree with Parmar et al., who found that the drug release from the lipid nanocarrier was affected by the degree of saturation of the phospholipid utilized in the fabrication of the lipid nanocarrier as the permeability of the bilayer was strongly influenced by its constituents where inclusion of saturated phospholipid within lipid bilayer increased its rigidity and consequently reduced the amount of drug released [42]. The regression coefficient values indicated that the in vitro release profile of all LPX formulae could best be fitted using the Higuchi release model.

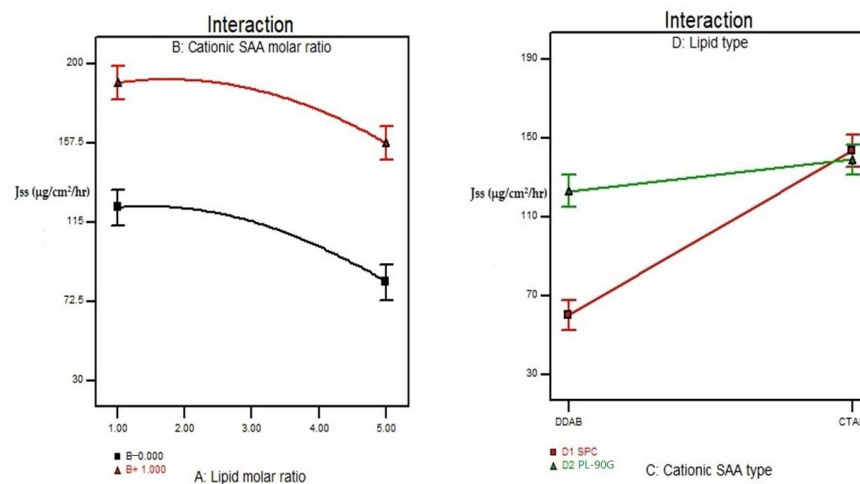


**Figure 4.** The effect of lipid molar ratio ( $X_1$ ), cationic surfactant molar ratio ( $X_2$ ), cationic surfactant type ( $X_3$ ), and lipid type ( $X_4$ ) on  $J_{ss}$ . Abbreviation:  $J_{ss}$ , steady-state flux.

### 3.7. Selection of the Optimized LPX Formula

To select the optimized LPX formula, specific parameters were set in Design Expert<sup>®</sup> software version 7. These conditions favored nanovesicles with the highest E.E.%, Z.P., Jss, and lowest P.S. and P.I. The optimized formula that met these criteria was composed of CTAB as cationic surfactant type and PL-G 90 as lipid type molar ratio of 1:0.67). The desirability of the optimized formula was 0.802, and it showed an E.E.% of  $85.2 \pm 0.95\%$ , P.S. of  $52.74 \pm 0.91$  nm, P.I. of  $0.21 \pm 0.02$ , Jss of  $175.03 \pm 1.68$   $\mu\text{g}/\text{cm}^2/\text{h}$ , and Z.P. of  $60.8 \pm 1.75$  mV. The predicted and observed responses of the optimized formula are shown in Table 3. A high correlation was observed between the observed and predicted values.

### 3.8. Morphology of the Optimized LPX Formula

The morphological examination of LPX evaluated by TEM clearly showed a spherical morphology with a uniform size distribution. The P.S. range was near that detected by the Zetasizer, as shown in Figure 5.

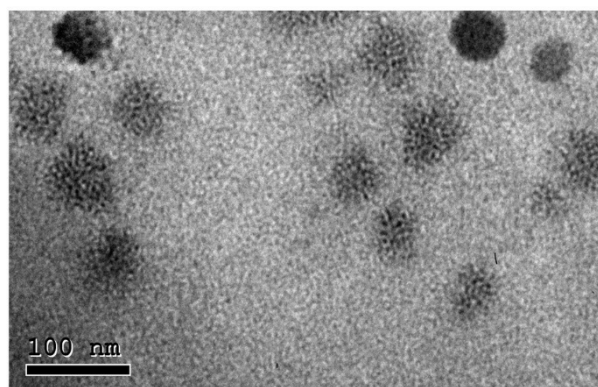


**Figure 5.** Morphology of the selected LPX. Abbreviation: LPX, lecplex.

### 3.9. Ex Vivo Permeation Study

The quantity of VAN permeated after 8 h ( $Q_8$ ) from the optimized LPX formula was significantly higher (unpaired *t*-test  $p < 0.05$ )  $404.62 \pm 1.95$  than from the free drug solution  $178.74 \pm 1.75$   $\mu\text{g}/\text{cm}^2$ , as shown in Table 4 and Figure 6, These results could be attributed to the reduced P.S. of the LPX formula ( $52.74 \pm 0.91$  nm), as it can create a high surface area for absorption. In addition, the positive charge of the nanovesicles mediates vesicle adhesion onto the negatively charged epithelial cell surfaces, consequently increasing the residence time and facilitating the endocytosis of vesicles [43]. Furthermore, the cationic surfactant interferes with the cellular lipid bilayer structure, facilitating drug uptake and opening tight bonds between epithelial cells. In the present study, the LPX formula enhanced the apparent permeability of VAN by 2.3-folds compared to the drug solution.

**Table 4.** Intestinal permeability parameters of VAN after application of VAN solution and LPX.

Intestinal Permeability Parameters	LPX	VAN Solution
The total amount of VAN permeated per unit area after 8 h ( $\mu\text{g}/\text{cm}^2$ )	$404.62 \pm 1.95$	$178.74 \pm 1.75$
Apparent permeability (cm/h)	$0.2240 \pm 0.0007$	$0.00970 \pm 0.0004$

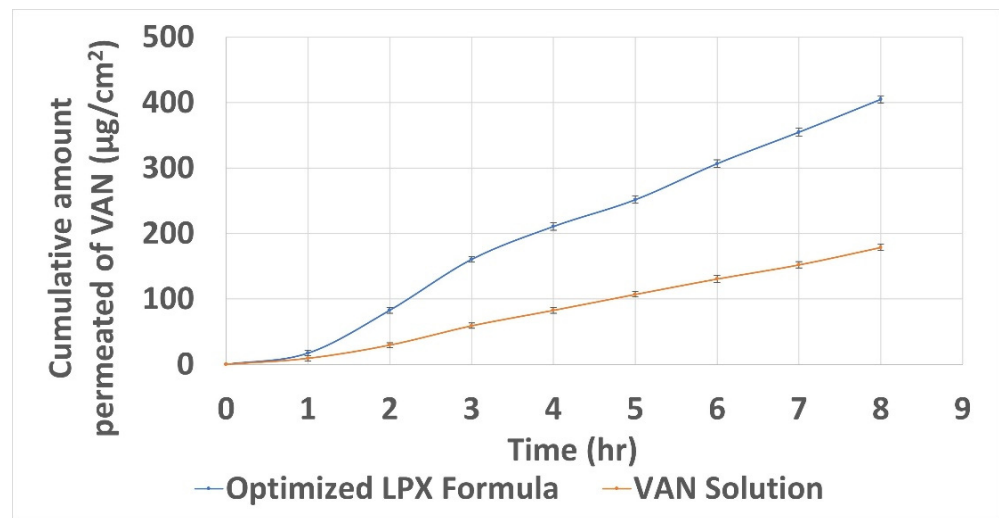


**Figure 6.** Cumulative amount permeated of VAN from the optimized LPX formula and aqueous solution. Abbreviations: VAN, Vancomycin hydrochloride; LPX, leciplex.

### 3.10. Differential Scanning Calorimetry

To further confirm the interaction between VAN and various LPX components, DSC thermograms were recorded for VAN, PL-90 G, CTAB, and the selected LPX formula Figure 7. The VAN thermogram showed a single broad peak at 83.4 °C, corresponding to the drug melting point. The thermogram of PL-90 G showed three somewhat broad peaks at 146, 174, and 265 °C. The CTAB thermogram showed two sharp endotherms in the tested temperature at 102.4 °C and 261 °C. The thermogram of the LPX showed three peaks at 111, 149, and 232 °C. The shifting of PL-90 G endotherm to lower temperature values might be due to the solubilization of PL-90 G with CTAB. These results confirmed the interaction of CTAB with the phospholipid portion of the LPX formula. Additionally, the absence of a VAN thermogram confirmed the drug’s complete encapsulation inside the cationic nanocarrier. These results agree with Beg et al., who reported that the vanishing of the semi-crystalline nature of the rosuvastatin in the DSC thermogram confirmed its encapsulation to the phospholipid-based nano lipospheres due to the formation of hydrogen bonds and van der Waal’s interaction forces between drug and PL-90 G [44].

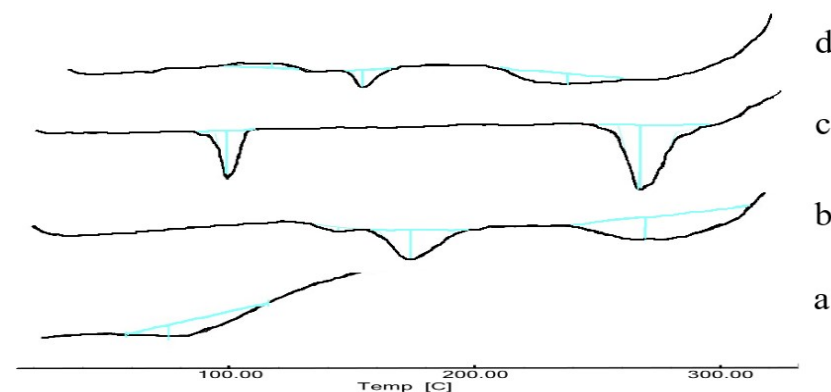


**Figure 7.** DSC thermograms; a, VAN; b, PL-90 G; c, CTAB; d, LPX formula. Abbreviations: DSC, differential scanning calorimetry; VAN, vancomycin hydrochloride; PL-90 G, phospholipon 90 G; CTAB, cetyltrimethylammonium bromide; LPX, leciplex.

### 3.11. Effect of Storage on the Selected LPX Formula

The physical stability of lipid vesicles is indirectly proportional to the vesicle size and directly proportional to the Z.P. of the dispersion. Aggregation of vesicles, representing poor stability, could be observed during formulation processing and/or upon storage. The visual inspection of the LPX formula did not demonstrate any sedimentation or vesicle aggregation during the storage period. In addition, E.E.%, P.S., P.I., and Z.P. measurements were  $84.6 \pm 0.41\%$ ,  $54.94 \pm 0.97$  nm,  $0.267 \pm 0.03$ , and  $60.6 \pm 0.41$  mV, respectively. These results showed insignificant variation from the freshly prepared LPX (paired *t*-test,  $p > 0.05$ ). These findings revealed the physical stability of the formulated LPX, which may be due to the CTAB that imparts a high positive charge on the nanocarrier surface. The charge of the nanovesicles is a fundamental property that can influence vesicular properties. Electrostatic repulsion can prohibit vesicles' mutual agglomeration and fusion and promote vesicle stability [30]. The stability of the VAN in the GIT environment is a critical factor for enhancing its oral bioavailability, as Uhl et al. correlated the improvement of VAN oral bioavailability with enhanced stability of VAN when loaded into tetraether lipid liposomes [45]. The amount of VAN retained within the LPX formula after incubation with SGF and SIF was  $85.2 \pm 1.67$  and  $92.6 \pm 0.98$  %, respectively; these results revealed that the cationic formula LPX had adequate stability in the harsh gastric-intestinal environment. These results agree with Data et al., who assumed that LPX could protect quercetin from enzymatic degradation in the GIT, resulting in greater bioavailability of the encapsulated drug [23].

### 3.12. Evaluation of Mucoadhesion Properties

After the addition of mucin to the cationic nanocarrier, a shift from the negative charge of mucin  $9.58$  mV  $\pm$   $0.53$  to a positive one of  $+9.09$  mV  $\pm$   $0.54$  was expected due to the interaction with cationic nanocarrier (LPX) and is an indication about the mucoadhesive properties of the LPX formula, such properties allow for it to adhere to the mucosal wall, increase the residence time and hence improve the drug absorption [46].

### 3.13. Cytotoxicity Assay

The *in vitro* toxicity (cell viability %) of the LPX formula, drug solution, and the positive control (Cis-Platin) were evaluated as described in the method section. The cell viability % of the LPX formula was not significantly different from the drug solution at each concentration (unpaired *t*-test,  $p > 0.05$ ), as shown in Figure 8. This result suggested that the LPX formula was well tolerated for oral drug delivery applications. These results are of great importance as several studies pointed to the cytotoxicity of the cationic surfactant; however, this cytotoxicity is concentration dependent and usually decreases after inclusion into the lipid bilayer [29].

### 3.14. In Vivo Assessment of the Selected LPX Formula

Figure 9 shows the plasma concentration versus time profile for the selected LPX formula and its comparison with VAN solution after oral administration in rats. The  $C_{\max}$  of VAN from LPX was significantly increased (unpaired *t*-test,  $p < 0.05$ ) by 2.99-fold ( $C_{\max}$ ,  $200.54 \pm 2.53$   $\mu\text{g}/\text{mL}$ ) compared to the VAN solution ( $C_{\max}$ ,  $67.00 \pm 1.95$   $\mu\text{g}/\text{mL}$ ).  $T_{\max}$  of VAN from the LPX formula and the VAN solution were 5 and 4 h, respectively. The higher  $T_{\max}$  value indicated the potential of the LPX formula to give sustained release.  $\text{AUC}_{0-t}$  was found to be  $1969.54 \pm 2.63$   $\mu\text{g}\cdot\text{h}/\text{mL}$  for LPX and  $576.11 \pm 1.21$   $\mu\text{g}\cdot\text{h}/\text{mL}$  for the aqueous solution. The MRT was  $44.13 \pm 1.83$  and  $19.5 \pm 1.28$  h for LPX and the VAN solution, respectively.

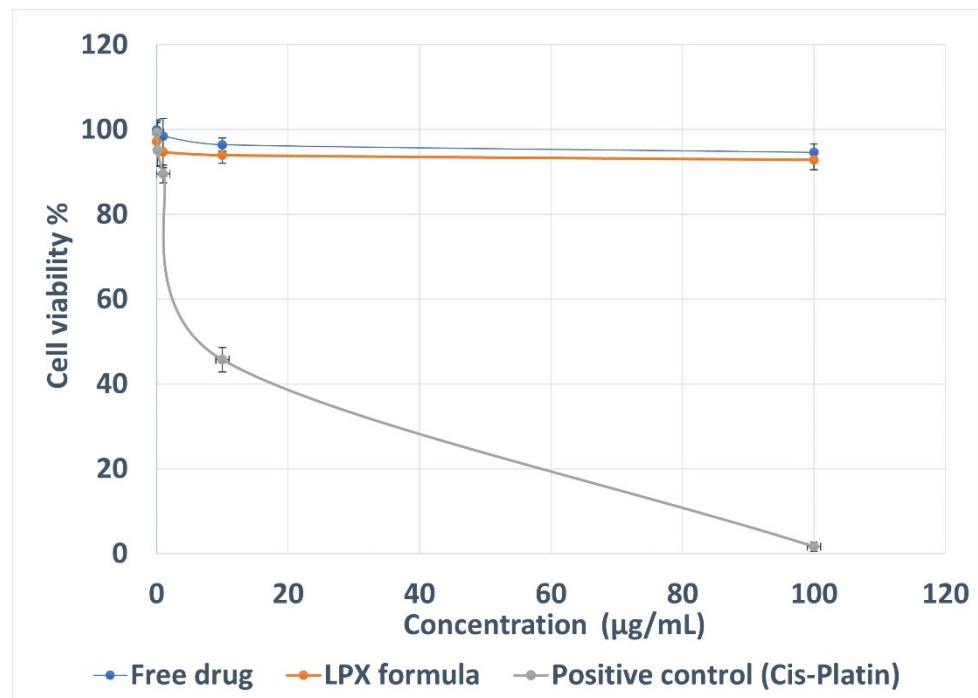


Figure 8. Cell viability percent using SRB colorimetric assay. Abbreviation: SRB, sulforhodamine B.

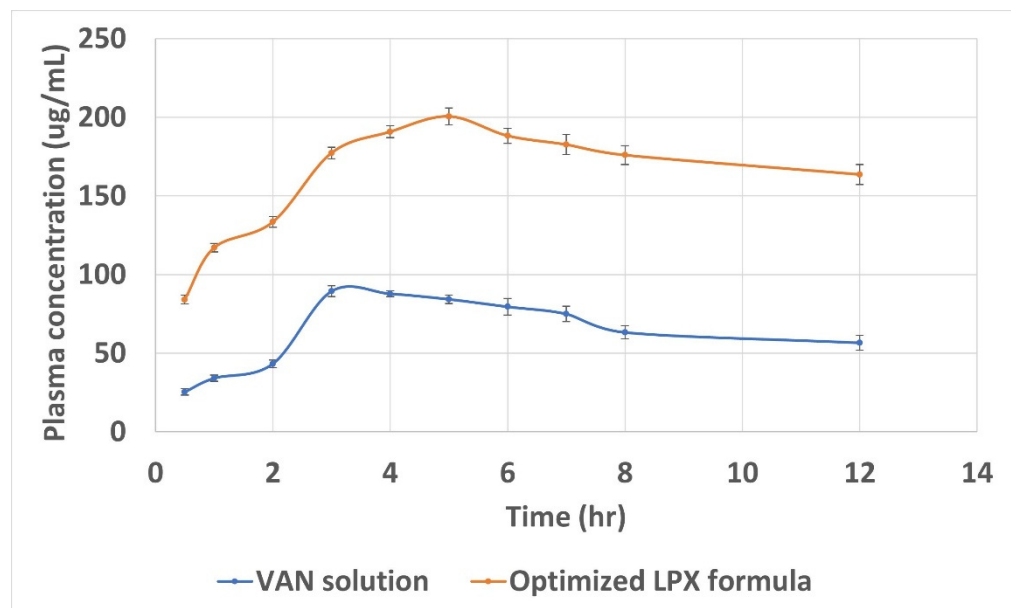


Figure 9. Mean plasma concentration-time curve of VAN following oral administration of the optimized LPX formula and VAN aqueous solution. Abbreviation: VAN, vancomycin hydrochloride; LPX, leciplex.

Drug transport across the intestinal epithelium is a complex and dynamic process that involves numerous mechanisms and pathways. Therefore, it is difficult to predict the predominate mechanism accurately. However, the enhanced intestinal absorption of VAN from the LPX formulae may be explained in terms of (a) enhanced stability of VAN inside the core of LPX against gastric microenvironment, (b) delivering the bio-enhancers with the drug together close to the absorption site, (c) altered permeability of the intestinal mucosa because of bio-enhancer, which promotes improved permeation of VAN across the gastric barrier via transcellular and paracellular, (d) mucoadhesion properties endows LPX with

prolonged GIT residence, allowing prolonged contact of LPX with intestinal epithelia and subsequently enhancing opportunities for oral absorption of VAN either encapsulated in the LPX or as free drug compared with free drug and ultimately resulting in enhanced passive permeation across intestinal epithelia, and (e) the reduced particle size and huge specific surface area of LPX.

The oral bioavailability improvement of hydrophilic macromolecule encapsulated into lipid vesicles depends on the fate of the vesicles after oral administration, where the stability of the vesicles in the GIT is a critical factor. Some of the orally administered lipid vesicles are destroyed in the acidic condition of the stomach, while the survival vesicles transit into the small intestine, where intestinal surfactants and enzymes destroy another fraction. The survival portion makes close contact with intestinal epithelia and contributes to the oral bioavailability enhancement of hydrophilic macromolecule drugs [47]. The positive charge of LPX might be contributed to the protection from GIT degradative processes and therefore play a role in VAN oral bioavailability enhancement. El-Naggar et al. found that cationic liposomes formulated for enhancing the oral bioavailability of the hydrophilic drug risedronate were more stable in SGF than anionic liposomes and concluded that it could be due to the expected high positive charge at this low pH value which would ensure strong repulsion between cationic vesicles and the attaching acids [48].

The role of the cationic surfactant as a bioenhancer in enhancing intestinal absorption of VAN is manifold in the following ways: (a) It interferes with cellular lipid bilayer structure, which leads to facilitated uptake of the released free drug; (b) it opens tight junctions and enhances absorption of released drug molecules; (c) it facilitates the uptake of the nanocarrier via endocytosis. Similar results were reported by Parmentier et al., who studied enhancing the oral bioavailability of fluorescein isothiocyanate (FITC)-dextran (hydrophilic macromolecule) via liposomal formulae modified with different bio-enhancers such as cetylpyridinium chloride and choly sarcosine in the presence of stearylamine, and found that the cationic surfactant cetylpyridinium chloride enhances the oral bioavailability of (FITC)-dextran via enhancing the cellular uptake (transcellular route) and opening the tight junction (paracellular routes) compared to the other bio-enhancers, and concluded that both pathways of permeation enhancement are theoretically possible for this formulation [49]. Furthermore, the cationic surfactant encouraged electrostatic interaction between the LPX and mucus layer, therefore facilitating the mucous adhesion of the LPX nanoparticles; this might prolong the residence time and drug contact with the underlying epithelium, thus increasing drug concentration at the site of absorption and consequently enhancing the absorption of VAN. In addition, the prolonged residence of lipid vesicles in the GIT increases the opportunity for uptake by M cells [24]. Furthermore, Yi et al. stated that mucoadhesion with epithelial cells favored the endocytosis of the nanovesicles, where the wrapping of membranes of the epithelial cells around the nanoparticle is dependent on the adhesive interaction between them [50].

It has been known that the reduced P.S. is essential for enhancing gastrointestinal absorption through endocytosis and paracellular pathways. Several systematic studies evaluating cellular uptake have been reported in the literature; they found that the cellular uptake was affected by various nanoparticle characteristics, including the nanoparticles' size, surface chemical structure, and shape. Most agreed that the smallest wrapping time depended on the particle size [51,52]. Furthermore, Delon et al. stated that paracellular transport allows only the passage of small particles [53]. Additionally, this reduced size can create a high surface area for absorption [54]. Despite the small population of M cells, this transport pathway might also enhance VAN intestinal permeability due to the reduced P.S. These results agree with Daeihamed et al., who stated that the P.S. of liposomes might also affect particle uptake by M-cells of Peyer's patches [55].

The phospholipid content in the LPX formula possesses both hydrophilic and lipophilic properties, similar to that observed in the phospholipid bilayer in human cells. These properties provided LPX with a specific advantage for increasing permeability by facilitating enhanced interactions between the drug and the cell membrane. Enhanced permeability

with phospholipid-based formula was achieved via one or more of the four mechanisms: adsorption, endocytosis, fusion, and lipid transfer [26].

Finally, the lipid-based nanocarrier LPX formula enhanced the oral bioavailability of a high molecular drug classified as class III; these results complied with previous studies that utilized lipid-based nanocarriers to enhance the oral bioavailability of hydrophilic drugs [56,57].

#### 4. Conclusions

The capability of cationic nanocarriers leciplex (LPX) to improve the oral bioavailability of the highly soluble and low permeable macromolecule drug (VAN) was successfully proven. Several overlapped mechanisms might be contributed to the enhancement of the VAN oral bioavailability, the protection from GIT enzymatic degradation with the presence of the bio-enhancer, the small particle size, and mucoadhesion properties. In addition, the molar ratio of the lipid and cationic surfactants with their types dramatically affected the properties of the prepared LPX. Finally, further studies are needed to elucidate the mechanisms of enhancing the oral bioavailability of hydrophilic macromolecules by LPX.

**Author Contributions:** Conceptualization, M.M.A., S.M.A., M.A.E.-N. and M.T.; methodology, M.M.A. and S.M.A.; software, M.M.A.; validation, M.M.A., S.M.A., M.A.E.-N. and M.T.; formal analysis, S.M.A.; investigation, S.M.A.; resources, M.M.A., S.M.A., M.A.E.-N. and M.T.; data curation, M.M.A.; writing—original draft preparation, M.M.A.; writing—review and editing, M.M.A., S.M.A., M.A.E.-N. and M.T.; supervision, M.M.A., M.A.E.-N. and M.T. All authors have read and agreed to the published version of the manuscript.

**Funding:** This research received no external funding.

**Institutional Review Board Statement:** The animal study protocol was approved by the Ethics Committee of the Faculty of Pharmacy, Cairo University (Approval NO.PI 2842, 28 December 2020).

**Informed Consent Statement:** Not applicable.

**Data Availability Statement:** Not applicable.

**Conflicts of Interest:** The authors declare no conflict of interest.

#### References

1. Maher, S.; Geoghegan, C.; Brayden, D.J. Intestinal permeation enhancers to improve oral bioavailability of macromolecules: Reasons for low efficacy in humans. *Expert Opin. Drug Deliv.* **2021**, *18*, 273–300. [[CrossRef](#)]
2. Gamboa, A.; Schüßler, N.; Soto-Bustamante, E.; Romero-Hasler, P.; Meinel, L.; Morales, J.O. Delivery of ionizable hydrophilic drugs based on pharmaceutical formulation of ion pairs and ionic liquids. *Eur. J. Pharm. Biopharm.* **2020**, *156*, 203–218. [[CrossRef](#)]
3. Phan, T.N.Q.; Shahzadi, I.; Bernkop-Schnürch, A. Hydrophobic ion-pairs and lipid-based nanocarrier systems: The perfect match for delivery of BCS class 3 drugs. *J. Control. Release* **2019**, *304*, 146–155. [[CrossRef](#)]
4. Deng, F.; Bae, Y.H. Bile acid transporter-mediated oral drug delivery. *J. Control. Release* **2020**, *327*, 100–116. [[CrossRef](#)]
5. Hodayun, B.; Lin, X.; Choi, H.-J. Challenges and Recent Progress in Oral Drug Delivery Systems for Biopharmaceuticals. *Pharmaceutics* **2019**, *11*, 129. [[CrossRef](#)]
6. Xu, Y.; Shrestha, N.; Pr eat, V.; Beloqui, A. An overview of in vitro, ex vivo and in vivo models for studying the transport of drugs across intestinal barriers. *Adv. Drug Deliv. Rev.* **2021**, *175*, 113795. [[CrossRef](#)]
7. Xu, Y.; Shrestha, N.; Pr eat, V.; Beloqui, A. Overcoming the intestinal barrier: A look into targeting approaches for improved oral drug delivery systems. *J. Control. Release* **2020**, *322*, 486–508. [[CrossRef](#)]
8. Zhu, Q.; Chen, Z.; Paul, P.K.; Lu, Y.; Wu, W.; Qi, J. Oral delivery of proteins and peptides: Challenges, status quo and future perspectives. *Acta Pharm. Sin. B* **2021**, *11*, 2416–2448. [[CrossRef](#)]
9. D unnhaupt, S.; Kammona, O.; Waldner, C.; Kiparissides, C.; Bernkop-Schn urch, A. Nano-carrier systems: Strategies to overcome the mucus gel barrier. *Eur. J. Pharm. Biopharm.* **2015**, *96*, 447–453. [[CrossRef](#)]
10. Ye, C.; Chi, H. A review of recent progress in drug and protein encapsulation: Approaches, applications and challenges. *Mater. Sci. Eng. C* **2018**, *83*, 233–246. [[CrossRef](#)]
11. Parmentier, J.; Hofhaus, G.; Thomas, S.; Cuesta, L.C.; Gropp, F.; Schr oder, R.; Hartmann, K.; Fricker, G. Improved Oral Bioavailability of Human Growth Hormone by a Combination of Liposomes Containing Bio-Enhancers and Tetraether Lipids and Omeprazole. *J. Pharm. Sci.* **2014**, *103*, 3985–3993. [[CrossRef](#)]
12. Ndayishimiye, J.; Cao, Y.; Kumeria, T.; Blaskovich, M.A.; Falconer, J.R.; Popat, A. Engineering mesoporous silica nanoparticles towards oral delivery of vancomycin. *J. Mater. Chem. B* **2021**, *9*, 7145–7166. [[CrossRef](#)]

13. Cerchiara, T.; Abruzzo, A.; Parolin, C.; Vitali, B.; Bigucci, F.; Gallucci, M.C.; Nicoletta, F.P.; Luppi, B. Microparticles based on chitosan/carboxymethylcellulose polyelectrolyte complexes for colon delivery of vancomycin. *Carbohydr. Polym.* **2016**, *143*, 124–130. [[CrossRef](#)]
14. Loveymi, B.D.; Jelvehgari, M.; Zakeri-Milani, P.; Valizadeh, H. Design of vancomycin RS-100 nanoparticles in order to increase the intestinal permeability. *Adv. Pharm. Bull.* **2012**, *2*, 43–56. [[CrossRef](#)]
15. Zakeri-Milani, P.; Loveymi, B.D.; Jelvehgari, M.; Valizadeh, H. The characteristics and improved intestinal permeability of vancomycin PLGA-nanoparticles as colloidal drug delivery system. *Colloids Surf. B Biointerfaces* **2013**, *103*, 174–181. [[CrossRef](#)]
16. Zaichik, S.; Steinbring, C.; Caliskan, C.; Bernkop-Schnürch, A. Development and in vitro evaluation of a self-emulsifying drug delivery system (SEDDS) for oral vancomycin administration. *Int. J. Pharm.* **2019**, *554*, 125–133. [[CrossRef](#)]
17. Efiana, N.A.; Dizdarević, A.; Huck, C.W.; Bernkop-Schnürch, A. Improved Intestinal Mucus Permeation of Vancomycin via Incorporation Into Nanocarrier Containing Papain-Palmitate. *J. Pharm. Sci.* **2019**, *108*, 3329–3339. [[CrossRef](#)]
18. Uhl, P.; Sauter, M.; Hertlein, T.; Witzigmann, D.; Laffleur, F.; Hofhaus, G.; Fidelj, V.; Tursch, A.; Özbek, S.; Hopke, E. Overcoming the Mucosal Barrier: Tetraether Lipid-Stabilized Liposomal Nanocarriers Decorated with Cell-Penetrating Peptides Enable Oral Delivery of Vancomycin. *Adv. Ther.* **2021**, *4*, 2000247. [[CrossRef](#)]
19. Maher, S.; Mrsny, R.J.; Brayden, D.J. Intestinal permeation enhancers for oral peptide delivery. *Adv. Drug Deliv. Rev.* **2016**, *106*, 277–319. [[CrossRef](#)]
20. Velpula, A.; Jukanti, R.; Janga, K.Y.; Sunkavalli, S.; Bandari, S.; Kandadi, P.; Veerareddy, P.R. Proliposome powders for enhanced intestinal absorption and bioavailability of raloxifene hydrochloride: Effect of surface charge. *Drug Dev. Ind. Pharm.* **2013**, *39*, 1895–1906. [[CrossRef](#)]
21. Babadi, D.; Dadashzadeh, S.; Osouli, M.; Daryabari, M.S.; Haeri, A. Nanoformulation strategies for improving intestinal permeability of drugs: A more precise look at permeability assessment methods and pharmacokinetic properties changes. *J. Control. Release* **2020**, *321*, 669–709. [[CrossRef](#)] [[PubMed](#)]
22. Kamel, R.; El-Deeb, N.M.; Abbas, H. Development of a potential anti-cancer pulmonary nanosystem consisted of chitosan-doped LeciPlex loaded with resveratrol using a machine learning method. *J. Drug Deliv. Sci. Technol.* **2022**, *70*, 103259. [[CrossRef](#)]
23. Date, A.A.; Nagarsenker, M.S.; Patere, S.; Dhawan, V.; Gude, R.P.; Hassan, P.A.; Aswal, V.; Steiniger, F.; Thamm, J.; Fahr, A. Lecithin-Based Novel Cationic Nanocarriers (LeciPlex) II: Improving Therapeutic Efficacy of Quercetin on Oral Administration. *Mol. Pharm.* **2011**, *8*, 716–726. [[CrossRef](#)] [[PubMed](#)]
24. He, H.; Lu, Y.; Qi, J.; Zhu, Q.; Chen, Z.; Wu, W. Adapting liposomes for oral drug delivery. *Acta Pharm. Sin. B* **2019**, *9*, 36–48. [[CrossRef](#)]
25. Cuomo, F.; Ceglie, S.; Miguel, M.; Lindman, B.; Lopez, F. Oral delivery of all-trans retinoic acid mediated by liposome carriers. *Colloids Surf. B Biointerfaces* **2021**, *201*, 111655. [[CrossRef](#)]
26. Dave, V.S.; Gupta, D.; Yu, M.; Nguyen, P.; Varghese Gupta, S. Current and evolving approaches for improving the oral permeability of BCS Class III or analogous molecules. *Drug Dev. Ind. Pharm.* **2017**, *43*, 177–189. [[CrossRef](#)]
27. Romes, N.B.; Wahab, R.A.; Abdul Hamid, M.; Hashim, S.E. D-optimal design-assisted *Elaeis guineensis* leaves extract in olive oil-sunflower seed nanoemulsions: Development, characterization, and physical stability. *J. Dispers. Sci. Technol.* **2022**, *43*, 289–301. [[CrossRef](#)]
28. Bhattacharya, S. Design and development of docetaxel solid Self-Microemulsifying drug delivery system using principal component analysis and D-Optimal design. *Asian J. Pharm.* **2018**, *12*, S122–S144.
29. Hassan, D.H.; Abdelmonem, R.; Abdellatif, M.M. Formulation and Characterization of Carvedilol LeciPlex for Glaucoma Treatment: In-Vitro, Ex-Vivo and In-Vivo Study. *Pharmaceutics* **2018**, *10*, 197. [[CrossRef](#)]
30. Albash, R.; Abdellatif, M.M.; Hassan, M.; Badawi, N.M. Tailoring Terpesomes and LeciPlex for the Effective Ocular Conveyance of Moxifloxacin Hydrochloride (Comparative Assessment): In-vitro, Ex-vivo, and In-vivo Evaluation. *Int. J. Nanomed.* **2021**, *16*, 5247–5263. [[CrossRef](#)]
31. Abdellatif, M.M.; Josef, M.; El-Nabarawi, M.A.; Teaima, M. Sertaconazole-Nitrate-Loaded LeciPlex for Treating Keratomycosis: Optimization Using D-Optimal Design and In Vitro, Ex Vivo, and In Vivo Studies. *Pharmaceutics* **2022**, *14*, 2215. [[CrossRef](#)] [[PubMed](#)]
32. Fong, S.Y.K.; Martins, S.M.; Brandl, M.; Bauer-Brandl, A. Solid Phospholipid Dispersions for Oral Delivery of Poorly Soluble Drugs: Investigation Into Celecoxib Incorporation and Solubility-In Vitro Permeability Enhancement. *J. Pharm. Sci.* **2016**, *105*, 1113–1123. [[CrossRef](#)]
33. Lavanya, N.; Muzib, Y.I.; Aukunuru, J.; Balekari, U. Preparation and evaluation of a novel oral delivery system for low molecular weight heparin. *Int. J. Pharm. Investig.* **2016**, *6*, 148–157. [[CrossRef](#)] [[PubMed](#)]
34. Allam, R.M.; Al-Abd, A.M.; Khedr, A.; Sharaf, O.A.; Nofal, S.M.; Khalifa, A.E.; Mosli, H.A.; Abdel-Naim, A.B. Fingolimod interrupts the cross talk between estrogen metabolism and sphingolipid metabolism within prostate cancer cells. *Toxicol. Lett.* **2018**, *291*, 77–85. [[CrossRef](#)] [[PubMed](#)]
35. Prasad, Y.V.R.; Puthli, S.P.; Eaimtrakarn, S.; Ishida, M.; Yoshikawa, Y.; Shibata, N.; Takada, K. Enhanced intestinal absorption of vancomycin with Labrasol and d- $\alpha$ -tocopheryl PEG 1000 succinate in rats. *Int. J. Pharm.* **2003**, *250*, 181–190. [[CrossRef](#)]
36. Date, A.A.; Srivastava, D.; Nagarsenker, M.S.; Mulherkar, R.; Panicker, L.; Aswal, V.; Hassan, P.A.; Steiniger, F.; Thamm, J.; Fahr, A. Lecithin-based novel cationic nanocarriers (LeciPlex) I: Fabrication, characterization and evaluation. *Nanomedicine* **2011**, *6*, 1309–1325. [[CrossRef](#)]

37. Salama, A.; Badran, M.; Elmowafy, M.; Soliman, G.M. Spironolactone-Loaded LeciPlexes as Potential Topical Delivery Systems for Female Acne: In Vitro Appraisal and Ex Vivo Skin Permeability Studies. *Pharmaceutics* **2020**, *12*, 25. [[CrossRef](#)]
38. Eroğlu, İ.; Azizoğlu, E.; Özyazıcı, M.; Nenni, M.; Güreer Orhan, H.; Özbal, S.; Tekmen, I.; Ertam, İ.; Ünal, İ.; Özer, Ö. Effective topical delivery systems for corticosteroids: Dermatological and histological evaluations. *Drug Deliv.* **2016**, *23*, 1502–1513. [[CrossRef](#)]
39. Therdpapiyanak, N.; Jaturanpinyo, M.; Waranuch, N.; Kongkaneramt, L.; Sarisuta, N. Development and assessment of tyrosinase inhibitory activity of liposomes of Asparagus racemosus extracts. *Asian J. Pharm. Sci.* **2013**, *8*, 134–142. [[CrossRef](#)]
40. Khatoon, K.; Rizwanullah, M.; Amin, S.; Mir, S.R.; Akhter, S. Cilnidipine loaded transfersomes for transdermal application: Formulation optimization, in-vitro and in-vivo study. *J. Drug Deliv. Sci. Technol.* **2019**, *54*, 101303. [[CrossRef](#)]
41. Ammar, H.O.; Tadros, M.I.; Salama, N.M.; Ghoneim, A.M. Ethosome-Derived Invasomes as a Potential Transdermal Delivery System for Vardenafil Hydrochloride: Development, Optimization and Application of Physiologically Based Pharmacokinetic Modeling in Adults and Geriatrics. *Int. J. Nanomed.* **2020**, *15*, 5671–5685. [[CrossRef](#)] [[PubMed](#)]
42. Parmar, J.J.; Singh, D.J.; Hegde, D.D.; Lohade, A.A.; Soni, P.S.; Samad, A.; Menon, M.D. Development and evaluation of inhalational liposomal system of budesonide for better management of asthma. *Indian J. Pharm. Sci.* **2010**, *72*, 442–448. [[CrossRef](#)] [[PubMed](#)]
43. Cao, S.-j.; Xu, S.; Wang, H.-m.; Ling, Y.; Dong, J.; Xia, R.-d.; Sun, X.-h. Nanoparticles: Oral Delivery for Protein and Peptide Drugs. *AAPS PharmSciTech* **2019**, *20*, 190. [[CrossRef](#)] [[PubMed](#)]
44. Beg, S.; Raza, K.; Kumar, R.; Chadha, R.; Katare, O.; Singh, B. Improved intestinal lymphatic drug targeting via phospholipid complex-loaded nanolipospheres of rosuvastatin calcium. *RSC Adv.* **2016**, *6*, 8173–8187. [[CrossRef](#)]
45. Uhl, P.; Pantze, S.; Storck, P.; Parmentier, J.; Witzigmann, D.; Hofhaus, G.; Huwyler, J.; Mier, W.; Fricker, G. Oral delivery of vancomycin by tetraether lipid liposomes. *Eur. J. Pharm. Sci.* **2017**, *108*, 111–118. [[CrossRef](#)]
46. Lin, Y.-J.; Shatkin, J.A.; Kong, F. Evaluating mucoadhesion properties of three types of nanocellulose in the gastrointestinal tract in vitro and ex vivo. *Carbohydr. Polym.* **2019**, *210*, 157–166. [[CrossRef](#)]
47. Sheikholeslami, B.; Lam, N.W.; Dua, K.; Haghi, M. Exploring the impact of physicochemical properties of liposomal formulations on their in vivo fate. *Life Sci.* **2022**, *300*, 120574. [[CrossRef](#)]
48. Elnaggar, Y.S.R.; Omran, S.; Hazzah, H.A.; Abdallah, O.Y. Anionic versus cationic bilosomes as oral nanocarriers for enhanced delivery of the hydrophilic drug risedronate. *Int. J. Pharm.* **2019**, *564*, 410–425. [[CrossRef](#)]
49. Parmentier, J.; Hartmann, F.J.; Fricker, G. In vitro evaluation of liposomes containing bio-enhancers for the oral delivery of macromolecules. *Eur. J. Pharm. Biopharm.* **2010**, *76*, 394–403. [[CrossRef](#)]
50. Yi, X.; Shi, X.; Gao, H. Cellular Uptake of Elastic Nanoparticles. *Phys. Rev. Lett.* **2011**, *107*, 098101. [[CrossRef](#)]
51. Xu, A.; Yao, M.; Xu, G.; Ying, J.; Ma, W.; Li, B.; Jin, Y. A physical model for the size-dependent cellular uptake of nanoparticles modified with cationic surfactants. *Int. J. Nanomed.* **2012**, *7*, 3547–3554. [[CrossRef](#)]
52. Gossman, R.; Langer, K.; Mulac, D. New perspective in the formulation and characterization of didodecyldimethylammonium bromide (DMAB) stabilized poly (lactic-co-glycolic acid)(PLGA) nanoparticles. *PLoS ONE* **2015**, *10*, e0127532. [[CrossRef](#)] [[PubMed](#)]
53. Delon, L.; Gibson, R.J.; Prestidge, C.A.; Thierry, B. Mechanisms of uptake and transport of particulate formulations in the small intestine. *J. Control. Release* **2022**, *343*, 584–599. [[CrossRef](#)] [[PubMed](#)]
54. Bajka, B.H.; Rigby, N.M.; Cross, K.L.; Macierzanka, A.; Mackie, A.R. The influence of small intestinal mucus structure on particle transport ex vivo. *Colloids Surf. B Biointerfaces* **2015**, *135*, 73–80. [[CrossRef](#)]
55. Daeihamed, M.; Haeri, A.; Ostad, S.N.; Akhlaghi, M.F.; Dadashzadeh, S. Doxorubicin-loaded liposomes: Enhancing the oral bioavailability by modulation of physicochemical characteristics. *Nanomedicine* **2017**, *12*, 1187–1202. [[CrossRef](#)]
56. Sheue Nee Ling, S.; Magosso, E.; Abdul Karim Khan, N.; Hay Yuen, K.; Anne Barker, S. Enhanced Oral Bioavailability and Intestinal Lymphatic Transport of a Hydrophilic Drug Using Liposomes. *Drug Dev. Ind. Pharm.* **2006**, *32*, 335–345. [[CrossRef](#)]
57. Palassi, S.; Valizadeh, H.; Allahyari, S.; Zakeri-Milani, P. Preparation and In Vitro Characterization of Enoxaparin Nano-liposomes through Different Methods. *Adv. Pharm. Bull.* **2021**, *11*, 295–300. [[CrossRef](#)]

**Disclaimer/Publisher's Note:** The statements, opinions and data contained in all publications are solely those of the individual author(s) and contributor(s) and not of MDPI and/or the editor(s). MDPI and/or the editor(s) disclaim responsibility for any injury to people or property resulting from any ideas, methods, instructions or products referred to in the content.